Zhou, H., Lu, Y., Zhang, M., Guerin, G., Manners, I., & Winnik, M. (2016). PFS-b-PNIPAM: A first step towards polymeric nanofibrillar hydrogels based on uniform fiber-like micelles. *Macromolecules*, *49*(11), 4265-4276. https://doi.org/10.1021/acs.macromol.6b00544

SUPPORTING INFORMATION

PFS-*b*-PNIPAM: A first step towards polymeric nanofibrillar hydrogels based on uniform fiber-like micelles

Hang Zhou[†], Yijie Lu[†], Meng Zhang[†], Gerald Guerin[*†], Ian Manners[‡], Mitchell A. Winnik[*†]

[†]Department of Chemistry, University of Toronto, Toronto, Ontario M5S 3H6, Canada
[‡]School of Chemistry, University of Bristol, Bristol BS8 1TS, United Kingdom

EXPERIMENTAL SECTION

1. Instrumentation

Gel Permeation Chromatography (GPC) measurements were carried out with a Waters 515 HPLC equipped with a Viscotek VE 3580 RI detector, and a 2500 UV-Vis detector in conjunction with poly(methyl methacrylate) standards. THF containing 2.5 g/L tetra-*n*-butylammonium bromide (TBAB) was used as the eluent (flow rate = 0.6 mL/min).

^{1}H NMR (500 MHz) spectra were recorded on an Agilent DD2 500 spectrometer with a 45^o pulse width and 10 s delay time at 25 ^{o}C. Solution turbidity was measured at 500 nm using a Perkin Elmer Lambda 35 UV/Vis spectrometer.

Transmission electron microscopy (TEM) measurements were performed on a Hitachi D-7000 microscope operating at an accelerating voltage of 100 kV operating in the bright-field TEM mode. Samples were prepared by placing a drop of solution on a Formvar-coated TEM grid and removing excess liquid with the edge of a filter paper. Images were analyzed with the software Image J (NIH, USA). A minimum of 100 individual fiber-like micelles were carefully traced by hand to determine the contour length. From this data L_n and L_w of each sample of cylindrical micelles was calculated as shown below (L = length of object, N = number).

$$L_n = \frac{\sum_{i=1}^{n} N_i L_i}{\sum_{i=1}^{n} N_i} \qquad L_w = \frac{\sum_{i=1}^{n} N_i L_i^2}{\sum_{i=1}^{n} N_i L_i} \qquad \text{(S1, 2)}$$

For a Gaussian shaped distribution, the standard deviations (σ) of the measured lengths are related to length dispersity (L_w/L_n) through the expression.

$$\frac{L_w}{L_n} - 1 = \left(\frac{\sigma}{L_n}\right)^2 \quad \text{(S3)}$$

2. Materials and Methods

The syntheses of 2-(2-azidoethoxy) ethyl bromoisobutyrate and alkyne terminated Poly(ferrocenylsilane) (DP_n = 26 and 56) were described in a previous publication.[1] N-isopropylacrylamide was recrystallized from hexane twice prior to use. CuBr was purified following a standard procedure[2] and stored in glove-box. All the other chemicals and solvents were used as received.

Azide-functionalized Poly(N-isopropylacrylamide). In a typical ATRP synthesis of PNIPAM, NIPAM (1.00 g, 8.86 mmol), CuBr (8.47 mg, 0.059 mmol), and Me_6TREN (13.57 mg, 0.059 mmol) dissolved in a 4 mL mixture of DMF: Water (v:v = 1:1) were introduced into a 25 mL Schlenk tube. After three cycles of freeze-pump-thaw, the azide-functionalized initiator 2-(2-Azidoethoxy) ethyl bromoisobutyrate (16.52 mg, 0.059 mmol) was introduced by a micro syringe at room temperature to start the polymerization. The reaction was run for 10 min and terminated by exposure to air and dilution with THF. An aliquot was removed for monomer conversion determination by NMR. Then the product was precipitated by injecting into 50 mL of diethyl ether under vigorous stirring followed by re-dissolving in THF and passing through an aluminum oxide column to remove the copper catalyst. Another two cycles of dissolution in THF and precipitation in ether gave samples of PNIPAM-N_3 that were then dried in a vacuum oven overnight. The polymer was subjected to GPC analysis (THF with 0.25 g/L tetra-*n*-butylammonium bromide as the eluent). For $PNIPAM_{190}$-N_3, **1**, Monomer conversion: 85%. ^{1}H NMR ($CDCl_3$, 400 MHz): δ (ppm, integrated peak areas reported are based on terminal methylene protons (4H, N_3-CH_2-C*H*$_2$-O-C*H*$_2$-CH_2-) as the reference) = 0.80-2.35 (broad, 9H, polymer backbone and two methyl groups, integration = 1835.2), 3.44 (t, 2H, N_3-C*H*$_2$-CH_2-O-CH_2-CH_2-, integration = 2.2), 3.71 (m, 4H, N_3-CH_2-C*H*$_2$-O-C*H*$_2$-CH_2-, integration = 4.0), 4.00 (broad, 1H, NH-C*H*-$(CH_3)_2$, integration = 189.1), 4.24 (t, 2H, N_3-CH_2-C*H*$_2$-O-C*H*$_2$-CH_2-, integration = 1.7), 5.50-7.00 (broad, 1H, N*H*-CH-$(CH_3)_2$, integration = 167.0). GPC (THF/TBAB, RI): M_n^{GPC} = 21.4 kDa, Đ = 1.06, DP_n = 190 ±10 (assuming 5% error from NMR integration), equivalent to M_n^{NMR} = 24 kDa.

For $PNIPAM_{520}$-N_3 **2**, GPC (THF/TBAB, RI): M_n^{GPC} = 59.9 kDa, Đ = 1.14. End-group determination by ^{1}H-NMR was inaccurate due to the low signal intensity of the end groups. To this end, we performed static light scattering measurements. Four polymer solutions in water were prepared (4.026, 6.068, 8.518, 10.37 mg/mL) and stored in a refrigerator (4 °C) overnight to ensure complete dissolution. Then all measurements were carried out at 23.00 ± 0.05 °C for 30s per scattering angle. The angular range investigated was from 30° to 150° (at 5° intervals). The weight-averaged molecular weight M_w was obtained from the Zimm plot relating the scattering vector q dependence of the excess absolute scattering intensity, the Rayleigh ratio R:

$$\frac{Kc}{R} = (1 + \frac{\langle R_g^2 \rangle q^2}{3})/M_w + 2A_2c \qquad \text{(S4)}$$

where $K = 4\pi^2 n^2 (dn/dc)^2/(N_A \lambda_0^4)$, $q = (4\pi n/\lambda_0)/\sin(\theta/2)$, and N_A, n, λ_0 and θ are the Avogadro number, the solvent refractive index, the wavelength of the light in vacuum, and the scattering angle, respectively. The Zimm plot (Figure S3) of Kc/R as a function of q^2+kc, was constructed using a value of k = 300. Extrapolation to zero concentration and zero scattering leads to M_w = 67 kDa). Thus $DP_n = M_w/(Đ \times M_{NIPAM})$ = 520.

Synthesis of PFS_{56}-b-$PNIPAM_{190}$ (3), and PFS_{26}-b-$PNIPAM_{520}$ (4). Diblock copolymers of PFS-*b*-PNIPAM were prepared via Cu-catalyzed alkyne azide cycloaddition (CuAAC) reaction between alkyne-terminated PFS and PNIAPM-N_3. Experimental details for PFS_{26}-*b*-$PNIPAM_{520}$ are provided below.

Alkyne terminated PFS_{26}-alkyne (35 mg, 5.0 μmol), $PNIPAM_{520}$-N_3 (180 mg, 3.0 μmol), and PMDETA (40 μL, 0.05 mmol) were dissolved in THF (4 mL) in a Schlenk tube. After three cycles of freeze-pump-thaw, the Schlenk tube was transferred to a N_2-protected glovebox followed by addition of CuBr (7.2 mg, 0.05 mmol). Then the reaction was allowed to stir at 40 °C for 4 days before being quenched by exposure to air. Aliquots of the mixture were removed before and after the reaction to monitor the reaction progress by GPC. The solution was then diluted with THF and passed through an Al_2O_3 column to remove the copper catalyst.

As indicated in the GPC curves after reaction (Figure S5), the block copolymers contained small amounts of unreacted PFS and PNIPAM homopolymer. To purify the diblock copolymer, the crude product was first subjected to three cycles of precipitation in water and redissolution in THF followed by centrifugation to isolate the insoluble block copolymer. Then the sediment was redissolved in small amount of THF (< 5 mL) and n-hexanes were added dropwise until the block

copolymer precipitated and the PFS homopolymers remained in the solvent. The solid was isolated by centrifugation and dried under vacuum overnight. Yield: 140 mg (67%). The polymer was analyzed by GPC (THF with 2.5 g/L tetra-*n*-butylammonium bromide as the eluent) and by NMR.

^{1}H NMR ($CDCl_3$, 400 MHz): δ (ppm, integrated peak areas reported are based on Cp protons (4H, Cp) as the reference) = 0.27-0.50 (broad, 6H, -Si(C*H*$_3$)$_2$-CP), 0.80-2.35 (broad, 9H, polymer backbone and two methyl groups), 3.85-4.19 (broad, 1H, NH-C*H*-(CH$_3$)$_2$, integration = 20), 3.85-4.35 (broad, 8H, Cp$_2$, integration = 8.0), 5.50-7.00 (broad, 1H, N*H*-CH-(CH$_3$)$_2$). GPC (THF/TBAB, RI): Mn^{GPC} = 81.6 kDa, Đ = 1.14. According to NMR, the block ratio of PFS and PNIPAM is 1:20, which also gives 520 as DP of PNIAPM.

Table S1. Summary of the polymer characteristics

Polymers	Theoretical M_n[a]	M_n^{NMR} [b]	M_n^{GPC}	Đ
PNIPAM$_{190}$-N$_3$	20.2 K	23.8 K	21.4 K	1.06
PNIPAM$_{520}$-N$_3$	34.1 K	65.0 K-	59.9 K	1.09
PFS$_{56}$-*b*-PNIPAM$_{190}$	-	39.7 K	39.4 K	1.11
PFS$_{26}$-*b*-PNIPAM$_{520}$	-	72.3 K	81.6 K	1.14

[a] Theoretical molecular weight was calculated by the equation:
M_n = [M]/[I]*$M_{monomer}$*Monomer Conversion + $M_{Initiator}$
[b] Calculated from DP_n

3. Micelle formation

Micelle preparation. Micelles were prepared by mixing block copolymer and solvent at a concentration of 0.2 mg/mL in a 7 mL vial. The vials were placed in an oil bath at 80 °C for 1 h, followed by slow cooling in which the oil bath was allowed to cool to room temperature (RT). Subsequently, the solutions were allowed to age for various times. Details for each solution are listed in Table S2. Figure 1 (main text) shows TEM images of PFS$_{56}$-*b*-PNIPAM$_{190}$ micelles in methanol, ethanol and 2-propanol solvents following aging for 1 day and 60 days. Figure 2 (main text) shows TEM images of fiber-like micelles of PFS$_{26}$-*b*-PNIPAM$_{520}$ in these three solvents after aging for three days.

Table S2. Summary of micelle preparation and shape

Polymers	Solvent [a]	Aging time	Results [b]
PFS_{56}-*b*-$PNIPAM_{190}$	Methanol	1 day	S
		60 days	S
	Ethanol	1 day	S
		60 days	S + C
	2-Propanol	1 day	S + C
		60 days	S + C
PFS_{26}-*b*-$PNIPAM_{520}$	Methanol	3 days	C
		7 days	C
	Ethanol	3 days	C
		7 days	C
	2-Propanol	3 days	C
		7 days	C

[a] The concentration of each solution is 0.2 mg/mL.
[b] S: Spherical micelles, C: Cylindrical micelles

Seeded growth. The long fiber-like micelle solutions of PFS_{26}-*b*-$PNIPAM_{520}$ (0.2 mg/mL in ethanol and 2-propanol) prepared as mentioned above was placed into a 70 watt ultrasonic cleaning bath and sonicated for 30 min at 23 °C to prepare seed solutions. An aliquot of the solution after sonication was taken for TEM analysis. Seed solutions were then diluted with the corresponding solvent to 20 μg/mL.

Three replicates of 2 mL of each seed solution were transferred to new vials for seeded growth experiments. Aliquots (8 μL, 20 μL and 32 μL) of PFS_{26}-*b*-$PNIPAM_{520}$ in THF (10 mg/mL), referred to as "unimer" solutions, were added into each seed solution and swirled for 10s. Every solution was allowed to age in the dark for at least 3 days before TEM measurements.

After forty days, the same seed solution and micelle solutions in ethanol and 2-propanol were measured again by TEM. The characteristics of these micelle samples varied by their unimer-to-

seed mass ratios and aging time, are summarized in Table S3. TEM images of these micelles are shown in Figure 3 and 4 (main text).

On the other hand, to confirm that all the unimers have deposited onto the micelles after aging for 40 days, the longest two micelle samples in ethanol and 2-propanol were re-characterized by TEM after aging for 90 days. Figure S6 compares the TEM images and length distribution histograms of these two samples.

Table S3. Summary of the characteristics determined by TEM of the micelles prepared by seeded growth of PFS_{26}-*b*-$PNIPAM_{520}$ in Ethanol and 2-Propanol

Solvent	Aging time	p[a]	L_n (nm)	L_w (nm)	L_w/L_n	σ/L_n
Ethanol	3 days	Seed	69.2	79.4	1.15	0.39
		2.0	204	213	1.04	0.21
		4.6	375	385	1.03	0.16
		7.3	552	563	1.02	0.15
	40 days	Seed’	83.8	90.4	1.08	0.28
		2.6	252	265	1.05	0.23
		5.8	474	488	1.03	0.17
		9.1	688	703	1.02	0.15
2-Propanol	3 days	Seed	101	108	1.06	0.25
		2.0	273	283	1.03	0.19
		4.8	503	512	1.02	0.14
		7.7	733	747	1.02	0.14
	40 days	Seed’	125	131	1.05	0.23
		2.7	364	377	1.04	0.19
		6.1	708	724	1.02	0.15
		9.7	1106	1122	1.01	0.12

[a] For data at 3 days aging, $p = p_{ex}$; whereas for data at 40 days aging, $p = p_{co}$. these parameters are defined in eqs 1 – 5 (main text).

4. Micelle characterization by light scattering

The rod-like micelles of different lengths prepared by seeded growth were diluted with corresponding solvent to concentrations in the range 5.5 - 5.8 μg/mL for light scattering measurements. Samples aged for both 3 days and 40 days were examined. All measurements were carried out at 23.00 ± 0.05 °C for 30 s (3 scans of 10s each). Three angular ranges were investigated. The first range consisted of scattering angles between 20° and 60° (at 2° intervals), second between 63° and 90° (at 3° intervals) and the last range consisted of angles between 95° and 150° (at 5° intervals). SLS and DLS measurements were carried out simultaneously. Filtered toluene was used as the standard solvent in the SLS experiments. In multi-angle static light scattering (SLS), we obtained structural and dimensional information by measuring the excess scattered intensity (known as the Rayleigh ratio, R_θ). For rigid rods of length L and cross section radius R_{SLS}, R_θ is related to concentration c, and the form factor $P(q)$ as expressed below:

$$f(q) = \frac{qR_\theta}{\pi M_0 Kc} = \frac{P(q)\cdot q}{\pi} \cdot L \cdot N_{agg/L} \tag{S6}$$

where

$$P(q, L, R_{SLS}) = \int_0^{\pi/2} \left(\left[2 \left(\frac{\sin\left(\frac{qL\cos\alpha}{2}\right)}{\frac{qL\cos\alpha}{2}} \right) \right] \frac{J_1(qR_{SLS}\sin\alpha)}{qR_{SLS}\sin\alpha} \right)^2 \sin\alpha \, d\alpha \tag{S7}$$

$K = 4\pi^2 n^2 (dn/dc)^2/(N_A \lambda_0^4)$, $q = (4\pi n/\lambda_0)/\sin(\theta/2)$, and N_A, n, λ_0 and θ are the Avogadro number, the solvent refractive index, the wavelength of the light in vacuum, and the scattering angle, respectively. For block copolymers, the specific refractive index increment $(dn/dc)_{polymer}$ is related to the dn/dc values of the components via the weight fractions w_j of monomer type j in the polymer (with $\sum_{j=1} w_j = 1$):

$$(dn/dc)_{polymer} = \sum_{j=1} w_j (dn/dc)_j \tag{S8}$$

provided that the dn/dc contributions of the multicomponent polymer in a single solvent are additive. Using values of $(dn/dc)_{PFS}$ = 0.253 mL/g and $(dn/dc)_{PNIPAM}$ = 0.136 mL/g in ethanol, $(dn/dc)_{PFS}$ = 0.240 mL/g and $(dn/dc)_{PNIPAM}$ = 0.119 mL/g in 2-propanol, we calculated $(dn/dc)_{polymer}$ = 0.148 and 0.131 mL/g in ethanol and 2-propanol, respectively. The SLS data were plotted as a Holtzer-Casassa (HC) plot of $qR_\theta/\pi M_0 Kc$ as a function of q and fitted according to equation S6 to get three parameters of the rod-like micelles: (i) the weight average length of the micelle L_w, (ii) the number of block copolymers per unit length of the micelles, a value we refer to as the linear

aggregation number, $N_{agg/L}$, and (iii) the radius of the cylinder cross section, R_{SLS}. In multi-angel dynamic light scattering (DLS), we measure the normalized intensity-intensity time-correlation function $[(g^{(2)}(q,\tau)-B)/B]$, where B is the measured baseline, τ is the decay time. $g^{(2)}(q,\tau)$ is related to the normalized electric field correlation function $g^{(1)}(q,\tau)$ by the Siegert relation:

$$g^{(2)}(\tau) = 1 + \beta\left|g^{(1)}(\tau)\right|^2 \tag{S9}$$

where β is a spatial coherence coefficient of the instrument. The Laplace inversion of $g^{(1)}(q,\tau)$ of scattering objects in a dilute solution can lead to a line-width distribution ($G<\Gamma>$). For a purely diffusive relaxation, for example of spherical particles, Γ is related to the translational diffusive coefficient (D) by $D = (\Gamma/q^2)_{q\to 0,\, c\to 0}$.

We first analyzed the data from individual scattering angles in terms of a cumulant expansion to second order (2-CUM) of the logarithm of $g^{(1)}(\tau)$, using the ALV correlator software:

$$\ln g^{(1)}(\tau) = -\Gamma_1\tau + \left(\frac{\mu_2}{2!}\right)\tau^2 \tag{S10}$$

where Γ_1 is also known as the first cumulant, μ_2 is the second cumulant. Examples of this fitting method are shown in Figure S10 with corresponding DLS autocorrelation decay profiles monitored at 34° of micelles in 2-propanol aged for 40 days. The evolution of Γ_1 is greatly influenced by the translational diffusion coefficient parallel, $D_\parallel$, and perpendicular, $D_\perp$, to the rod axis, and by the rotational diffusion coefficient, D_r, as a function of the scattering angle. For a dilute solution of rigid rods, when the translational and rotational motions are coupled, Wilcoxon and Schurr have shown that Γ/q^2 can be expressed by eq S11:

$$\frac{\Gamma_1}{q^2} = \left[D + 2(D_\parallel - D_\perp)\cdot\left(\frac{1}{3} - F(qL)\right) + 2L^2 D_r G(qL)\right] \tag{S11}$$

where D is the overall translational diffusion coefficient of the rod, defined as $D = (2\,D_\perp + D_\parallel)/3$. $F(qL)$ and $G(qL)$ are universal functions of qL, which are defined in terms of readily evaluated sums:

$$F(qL) \equiv SUM2/SUM1 \tag{S12}$$

$$G(qL) \equiv N^{-2}SUM3/SUM1 \tag{S13}$$

where

$$SUM1 \equiv N^2\,\frac{1}{(qL)^2}\iint_{-qL/2}^{qL/2}\frac{\sin|x-y|}{|x-y|}\,dxdy \tag{S14}$$

$$SUM2 \equiv N^2 \frac{1}{(qL)^2} \iint_{-qL/2}^{qL/2} \left\{ \frac{\sin|x-y|}{|x-y|^3} - \frac{\cos|x-y|}{|x-y|^2} \right\} dxdy \quad \text{(S15)}$$

$$SUM3 \equiv N^4 \frac{1}{(qL)^4} \iint_{-qL/2}^{qL/2} xy \left\{ \frac{\sin|x-y|}{|x-y|^3} - \frac{\cos|x-y|}{|x-y|^2} \right\} dxdy \quad \text{(S16)}$$

with N identical scattering elements arranged in a linear sequence of a thin rigid rod.

The translational and rotational diffusion coefficients can be expressed as a function of the ratio of the rod length to the cross-sectional diameter, L/d, and the solvent viscosity, η_0. [3–5] These values are evaluated according to the boundary element method (BE) developed by Aragon and Flamik, where the PFS rods are best represented by cylinders with flat caps.[6]

For cylinders with flat caps, the translational diffusion coefficients, $D_\parallel$ and $D_\perp$, are given by[7]

$$D_\parallel = \frac{kT}{4\pi\eta_0 L}\left(2ln\left(\frac{L}{d}\right) + X_\parallel\right) \quad \text{(S17a)}$$

$$D_\perp = \frac{kT}{4\pi\eta_0 L}\left(ln\left(\frac{L}{d}\right) + X_\perp\right) \quad \text{(S17b)}$$

where

$$X_\parallel\left(\frac{L}{d}\right) = -0.234963 - \frac{3.14268}{\sqrt{L/d}} + \frac{4.29031}{L/d} + \frac{0.197913}{(L/d)^2} + \frac{1.96581\ln(L/d)}{(L/d)^2} \quad \text{(S18a)}$$

$$X_\perp\left(\frac{L}{d}\right) = 0.866049 - \frac{0.650602}{\sqrt{L/d}} + \frac{1.2839}{L/d} - \frac{0.397905}{(L/d)^2} - \frac{0.18332\ln(L/d)}{(L/d)^2} \quad \text{(S18b)}$$

and the rotational diffusion coefficient D_r is given by

$$D_\mathrm{r} = \frac{3kT}{\pi\eta_0 L^3}\left(ln\left(\frac{L}{d}\right) + X_\mathrm{r}\right) \quad \text{(S19)}$$

where

$$X_\mathrm{r}\left(\frac{L}{d}\right) = -0.480483 - \frac{1.40054}{\sqrt{L/d}} - \frac{3.91903}{L/d} - \frac{2.4528}{(L/d)^3} + \frac{0.587033}{(L/d)^4} - \frac{2.58127\ln(L/d)}{(L/d)^2} \quad \text{(S20)}$$

By varying the value of d (cross-sectional diameter), one can fit the plot of Γ/q^2 as a function of qL to get the hydrodynamic radius R_DLS for each micelle solution.

The structural parameters of the micelles after 40 days aging are described in the main text. Corresponding information for the micelles obtained after only 3 days aging, by TEM and light scattering, are summarized in Table S4. Since the solutions examined after 3 days aging is a mixture of micelles and unimer, both of them contribute to the scattering intensity, $\frac{R_\theta}{K}$:

$$\frac{R_\theta}{K} = P(q)_{micelle} M_{micelle} c_{micelle} + P(q)_{unimer} M_{unimer} c_{unimer} \quad \text{(S21)}$$

where *P(q), M* and *c* refer to the form factor, weight-averaged molecular weight and concentration of each species. $M_{micelle}$ is given by the product of the micelle length, the linear aggregation number and the unimer molecular weight ($L \times N_{agg,L} \times M_{unimer}$). The second term of eq S21 becomes insignificant as $M_{micelle}$ is hundreds time larger than M_{unimer}. Thus we consider the signal contribution from the micelles equals to the total scattering intensity. The SLS data of the samples aged for three days were analyzed by replacing *c* in eq S6 with $c_{micelle}$, given by:

$$c_{micelle} = \frac{L_3}{L_{40}} \times c \tag{S22}$$

where *c* corresponds to the total amount of polymer (micelles + unimer) present in the solution.

Table S4. Summary of structural parameters characterized by TEM and light scattering of micelles aging for three days

Solvent	p_{ex}	$L_{w,3\ TEM}$ (nm)	$L_{w,3\ SLS}$ (nm)	$N_{agg,L}$ (chains/nm)	R_{SLS} (nm)	R_{DLS} (nm)
Ethanol	2.0	213	225	1.12	17	29
	4.6	385	350	1.11	17	31
	7.3	564	520	1.07	17	31
2-Propanol	2.0	283	285	0.86	17	33
	4.8	512	520	0.89	17	33
	7.7	747	740	0.94	17	35

The values of $N_{agg,L}$ in Table S4 are somewhat larger than those presented in Table 1 of the main text. We do not consider these differences to be significant because the magnitude of $N_{agg,L}$ is rather sensitive to the exact value (*c* or $c_{micelle}$) introduced into the Holtzer-Casassa (HC) plots of $qR_\theta/\pi M_0 Kc$ as a function of *q*. Values of *c*, appropriate for samples aged 40 days, are known precisely from the details of sample preparation, whereas values of $c_{micelle}$ require a correction according to eq S22.

5. Phase diagram of PNIPAM in water/2-propanol mixture

Two solutions of PNIPAM in water and 2-propanol (2 mg/mL) were prepared and kept in a refrigerator overnight for complete dissolution. At room temperature, different amounts of each solution were withdrawn and mixed (total volume around 1 mL) in well-defined water/2-propanol

ratios and equilibrated for 10 min before testing the turbidity of each solution at 500 nm. The results are presented in Figure S10.

6. Tests of the thermoresponsiveness of fragmented micelles in water

After injection of 0.1 mL of the longest micelle sample (m_{unimer}/m_{seeds} = 9.7) in 2-propanol into 1.9 mL water, the solution was concentrated slowly by placing the half-opened vial in a desiccator connected to a water aspirator. The final volume of the solution was ca. 0.1 mL (c = 0.18 mg/mL). Temperature-dependent micelle turbidity measurements at 500 nm using a UV-Vis spectrometer showed no significant changes for samples at 25 ºC, 30 ºC, 32 ºC, 35 ºC, 40 ºC and 45 ºC. To test whether subjecting the sample to a heating-cooling cycle affected the length of the micelle fragments, a drop of the sample heated to 45 °C and cooled to RT was placed on a TEM grid for TEM image analysis. The resulting micelle length distribution was compared with that of a corresponding sample that was not heated. TEM images and length distribution histogram are presented in Figure S11.

Temperature-dependent DLS measurements were carried out with the same micelle sample in water on a Malvern Nano ZS Zetasizer (173° scattering angle) at 25, 30, 35, 40 and 45 ºC. The sample in the sample chamber takes ca. 2 min to reach the target temperature. Then the sample was equilibrated at that temperature for 2 min before acquiring signals. Three consecutive measurements of 11 runs, 15 seconds each, were taken for each temperature (Each measurement took c.a. 3 mins). Figure S13 shows the autocorrelation functions of measurement at various temperatures along with the CONTIN plots.

SUPPORTING FIGURES

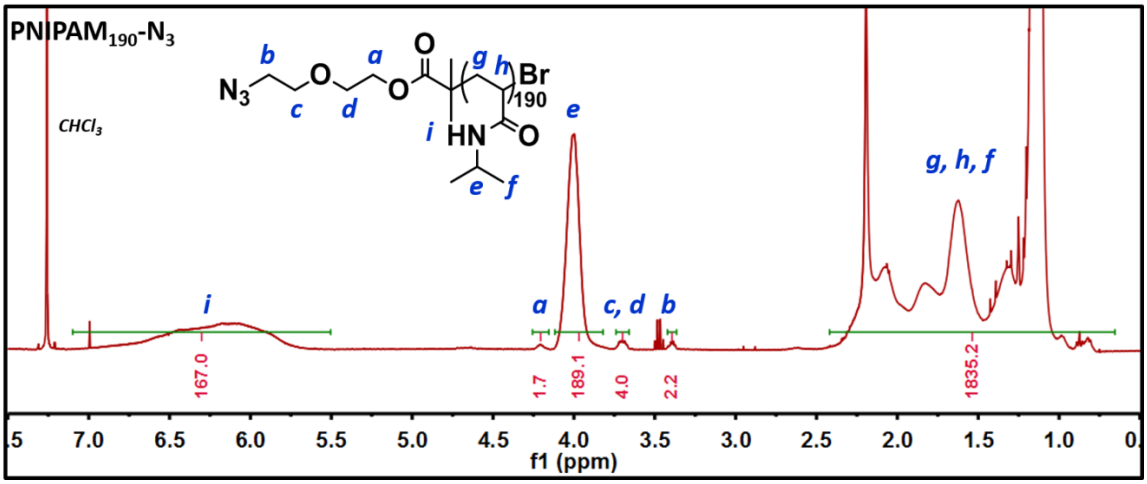

Figure S1. ^{1}H-NMR of PNIPAM$_{190}$-N$_3$ (in CDCl3). End group analysis, comparing the integration of the CH2-O signals (a), (b), and (c,d) on the ATRP initiator to those of the signals from the isopropyl groups (e) on the polymer gave DPn = 190.

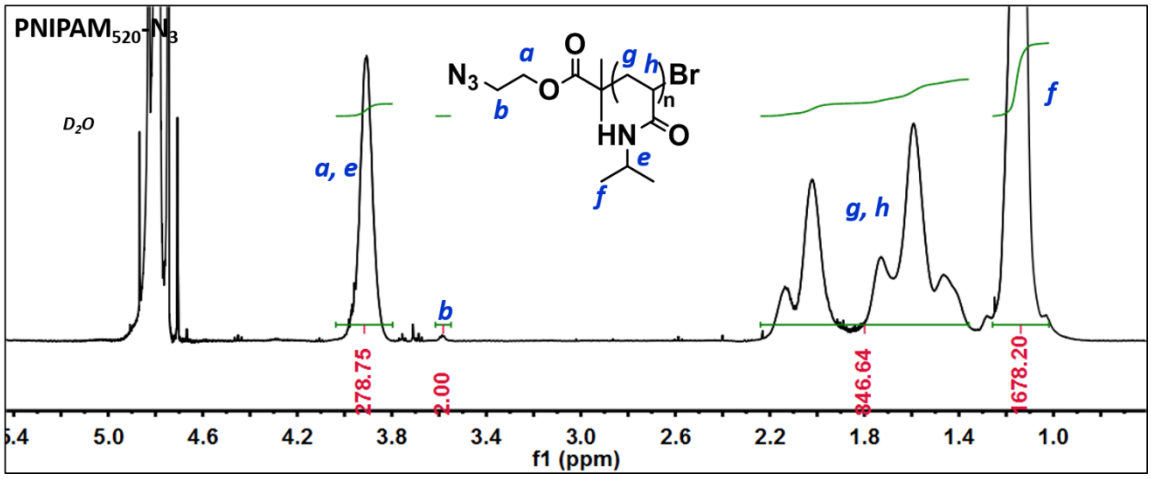

Figure S2. ^{1}H-NMR of PNIPAM$_{520}$-N$_3$ (in D$_2$O). End group analysis did not give an accurate DPn due to poor signal to noise ratio of the end group (b) from the ATRP initiator.

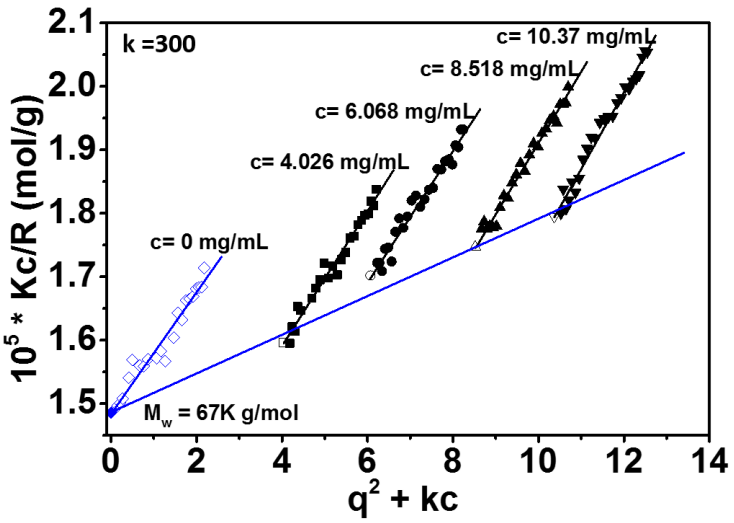

Figure S3. Zimm plot of PNIPAM$_{520}$-N$_3$ measured in water at room temperature; where *c* ranges from 4 to 10 mg/mL as shown in the plot (k = 300)

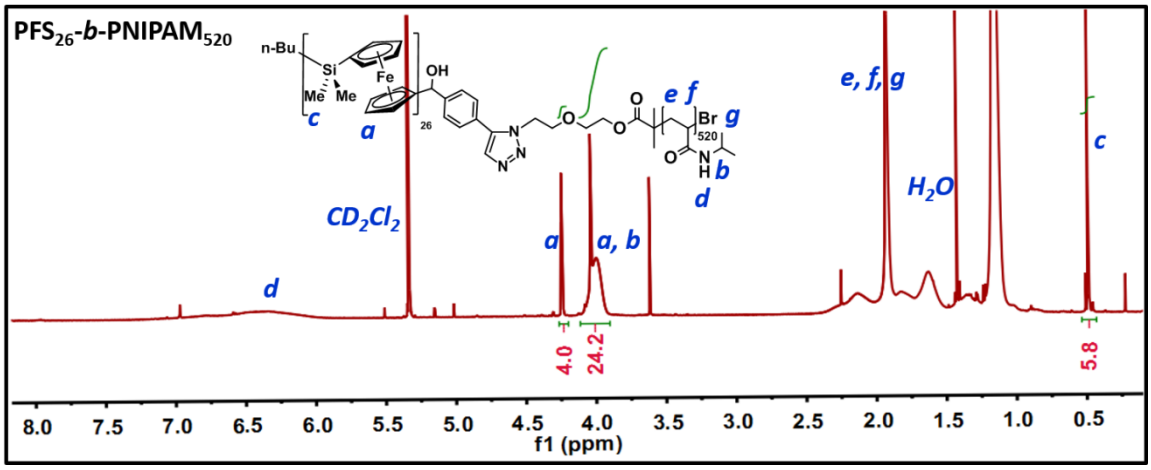

Figure S4. ^{1}H-NMR of PFS$_{26}$-*b*-PNIPAM$_{520}$ (in CD_2Cl_2). Comparing the integration of protons from the Cp rings (a) and isopropyl groups (b) gave the block ratio of 1: 20, which resulted in the DPn of PNIPAM = 26*20 = 520.

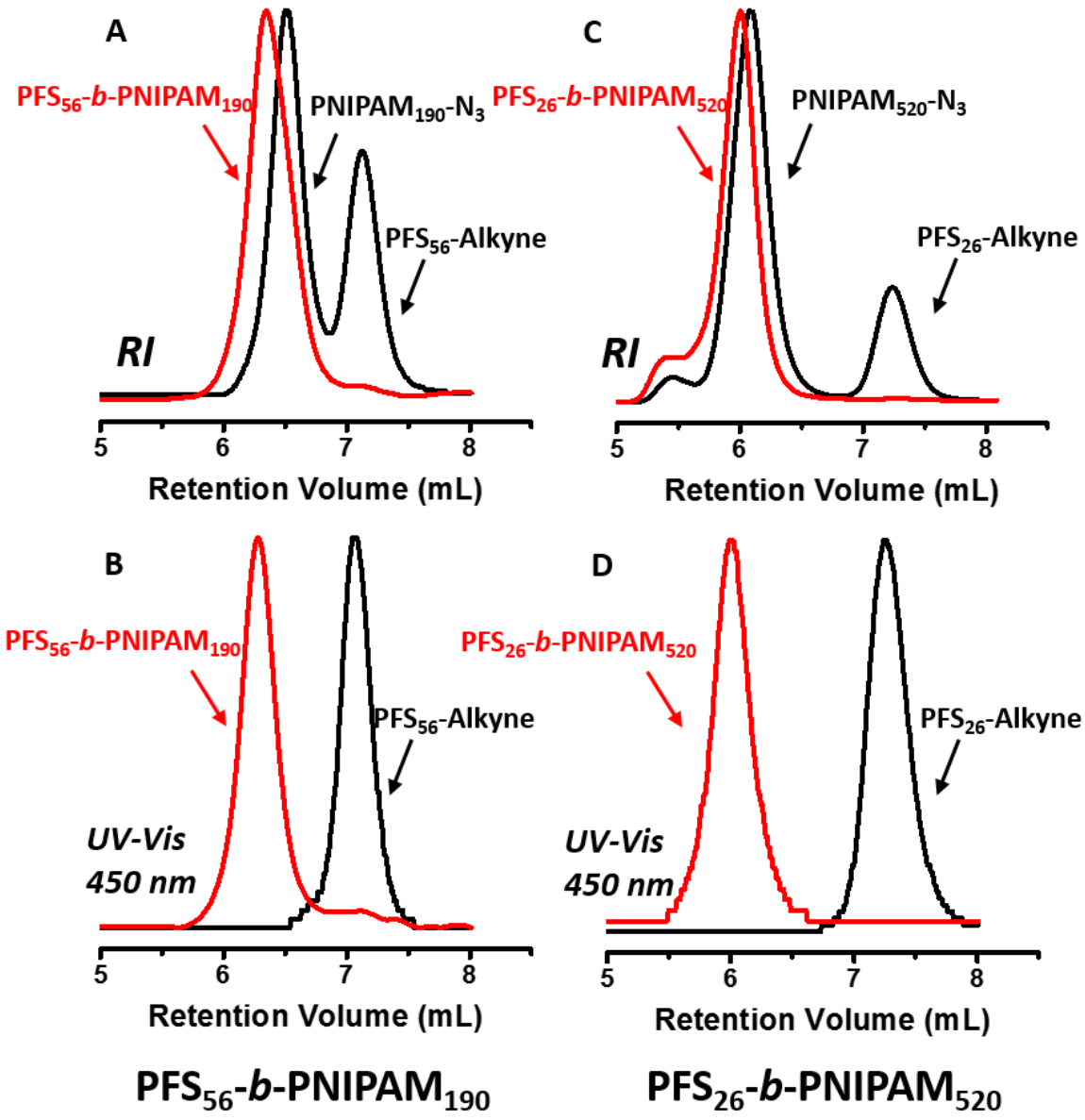

Figure S5. GPC curves before (black lines) and after (red lines) click reaction of PFS-Alkyne and PNIPAM-N_3 in THF (A) RI signal and (B) UV-Vis signal (UV-Vis detector wavelength: 450 nm) of PFS_{56}-*b*-$PNIPAM_{190}$. (C) RI signal and (D) UV-Vis signal (UV-Vis detector wavelength: 450 nm) of PFS_{26}-*b*-$PNIPAM_{520}$.

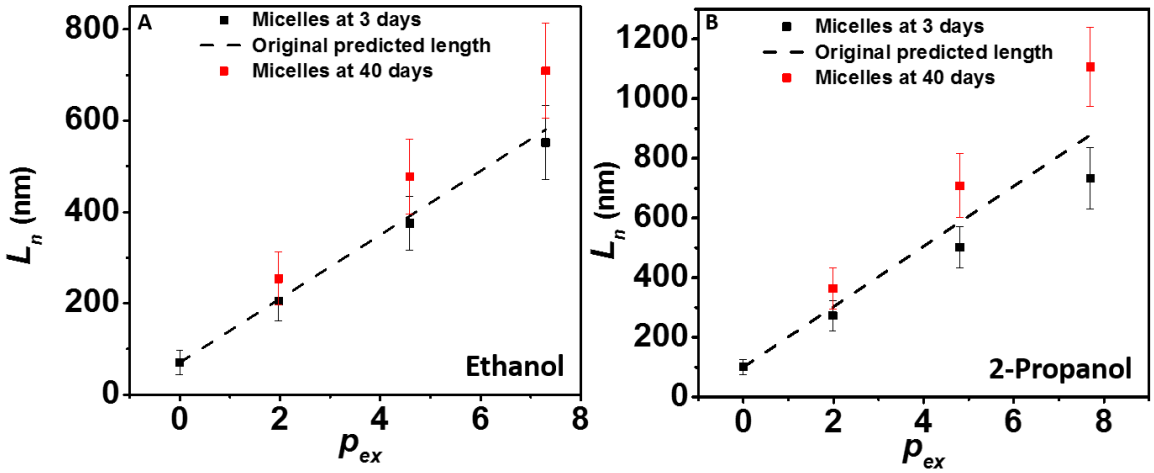

Figure S6. Number average length L_n obtained by the seeded growth experiment versus the ratio of the amount of PFS_{26}-*b*-$PNIPAM_{520}$ added in ethanol (A) and 2-propanol (B) after three days aging. The dashed line represents the predicted maximum lengths based on eq. **1**. The red points represent the number average lengths of the micelles aged for 40 days.

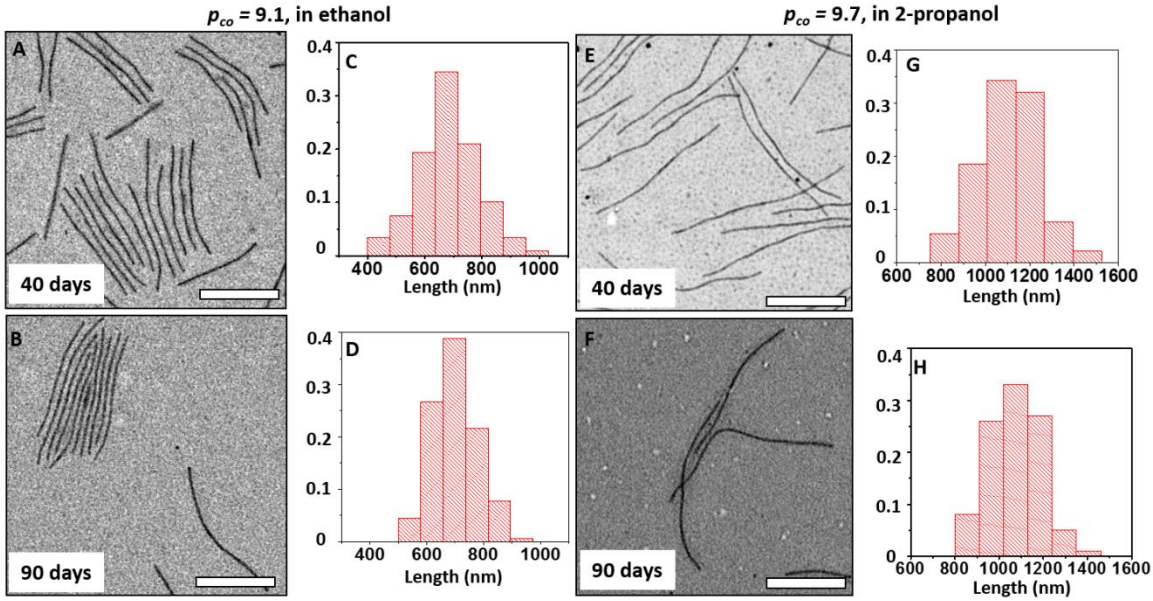

Figure S7. Comparison of the TEM images and length histograms of the longest micelles in ethanol after aging for 40 days (A, C) and 90 days (B, D) , as well as in 2-propanol aging for 40 days (E, G) and 90 days (F, H) confirms no further micelle growth beyond 40 days. Scale bars: 500 nm

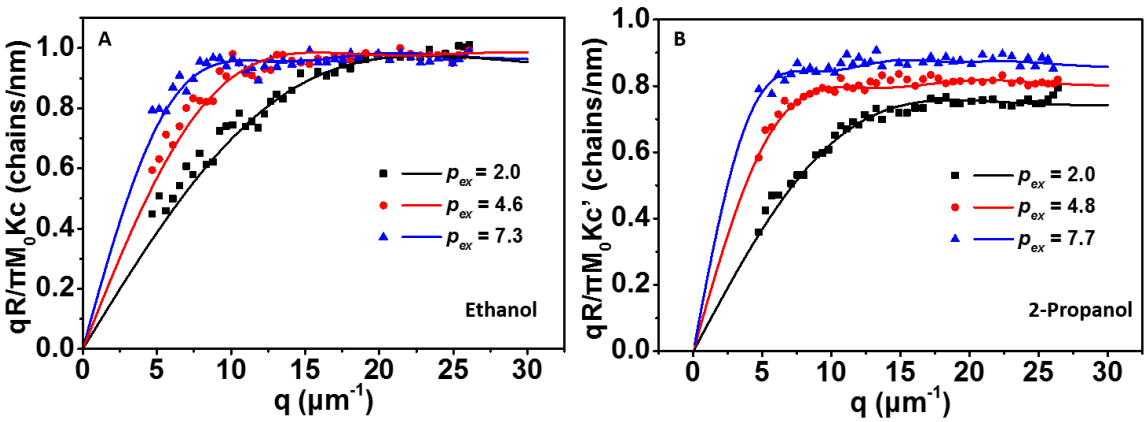

Figure S8 Holtzer-Casassa plots of $qR_\theta/\pi M_0 Kc$ as a function of q for the micelles in ethanol (A) and 2-propanol (B) after aging for 3 days. The concentrations are corrected based on the micelle lengths at 40 days characterized by TEM. The data points of different colors represent micelles of different lengths indicated by the expected p values before correction (p_{ex}). Each line represents the best fit of the corresponding data set to eq S6 for thick rigid rods.

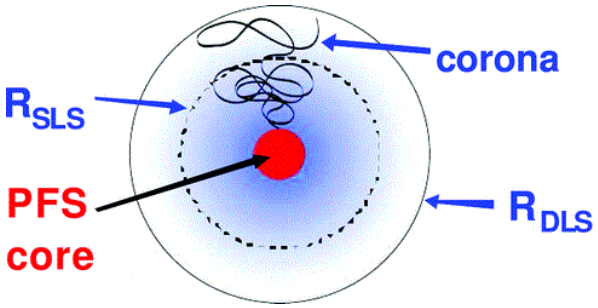

Figure S9 Schematic representation of the cross section of rod-like PFS-*b*-PNIPAM micelles indicting the meaning of the two characteristic radii determined by multi-angle light scattering.[7]

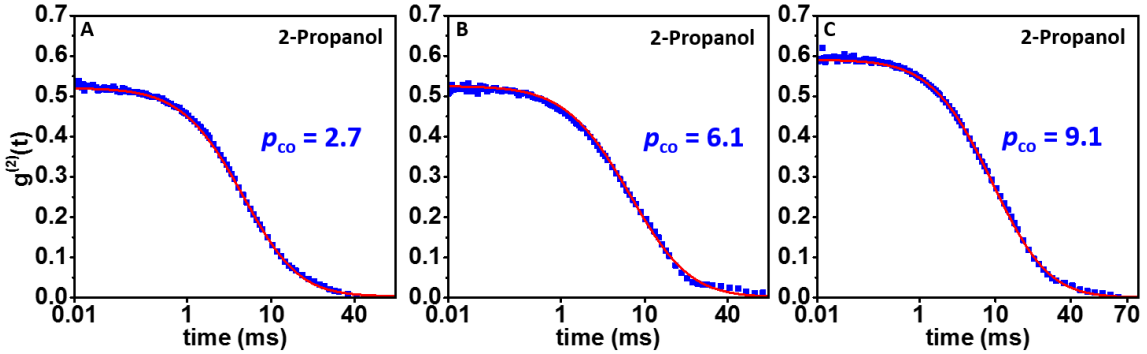

Figure S10. DLS autocorrelation decay profiles monitored at 34° (blue squares) for micelles aged for 40 days in 2-propanol for a ratio p_{co} of (A) 2.7, (B) 6.1, and (C) 9.1. Each decay could be well fitted by a second-order cumulant equation (eq S11, red lines)).

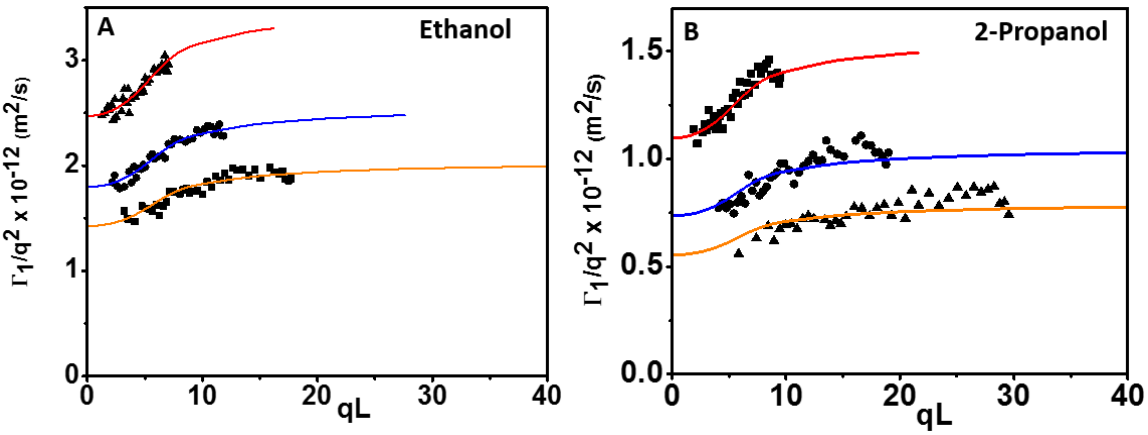

Figure S11. Plots of Γ_1/q^2 as a function of qL for the micelles in ethanol (A) and 2-propanol (B) after aging for 40 days. The L value corresponds to L_w from SLS data. The lines correspond to the best fits obtained from eq S11.

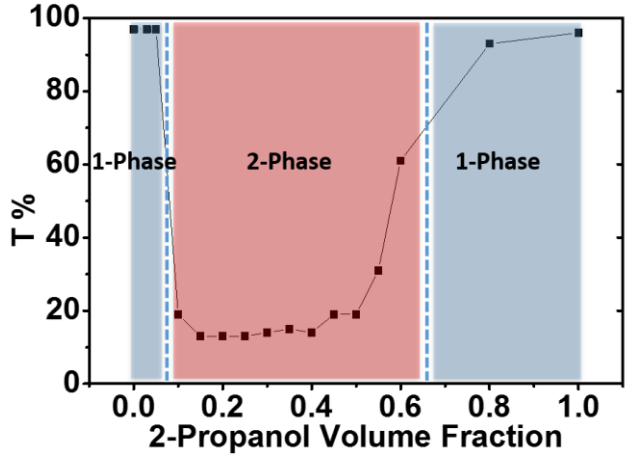

Figure S12. Turbidity of PNIPAM solutions in water/2-propanol mixtures at 25 °C by UV-Vis measurements at 500 nm. c = 2 mg/mL.

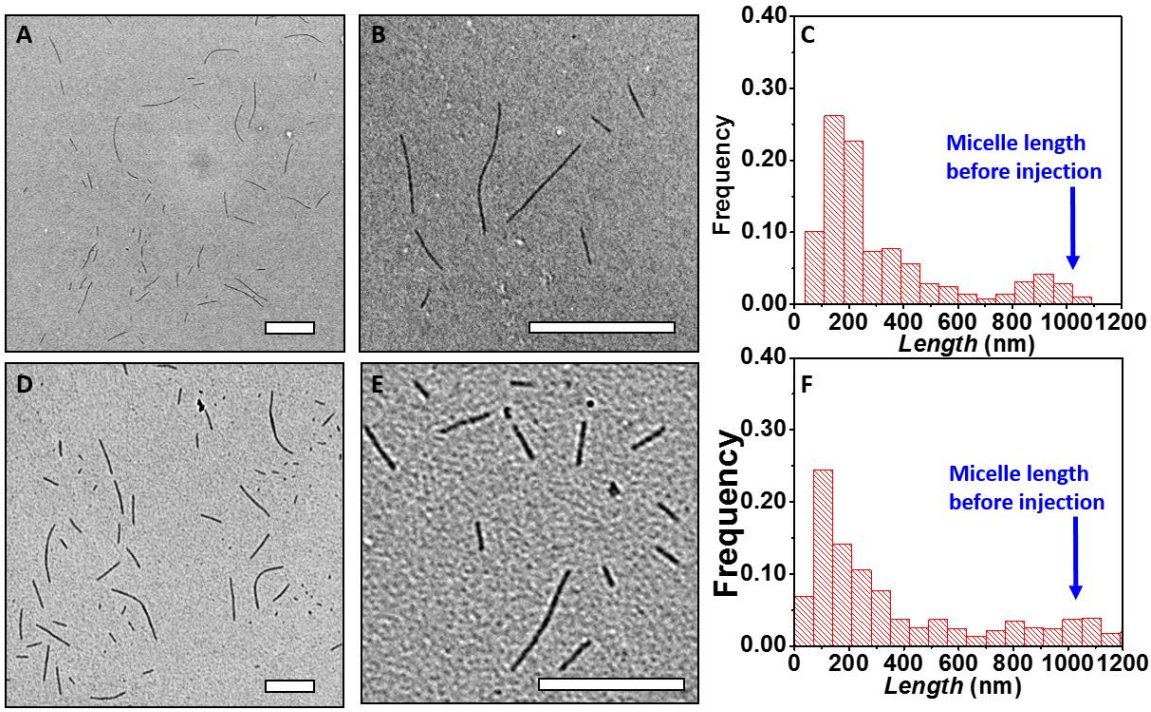

Figure S13. (A, B) TEM images of fragmented micelles after injection into water from 2-propanol (water/2-propanol v:v = 19:1) Scale bars: 500 nm. (C) Length distribution histogram of the fragmented micelles. Blue arrow indicates the length of the micelle before transferring. (D, E) TEM images of fragmented micelles in water after heating to 45 °C for 2 mins and cooling slowly to room temperature. (F) Length distribution histogram of the fragmented micelles after one heat-cool cycle. Blue arrow indicates the length of the micelle before transferring.

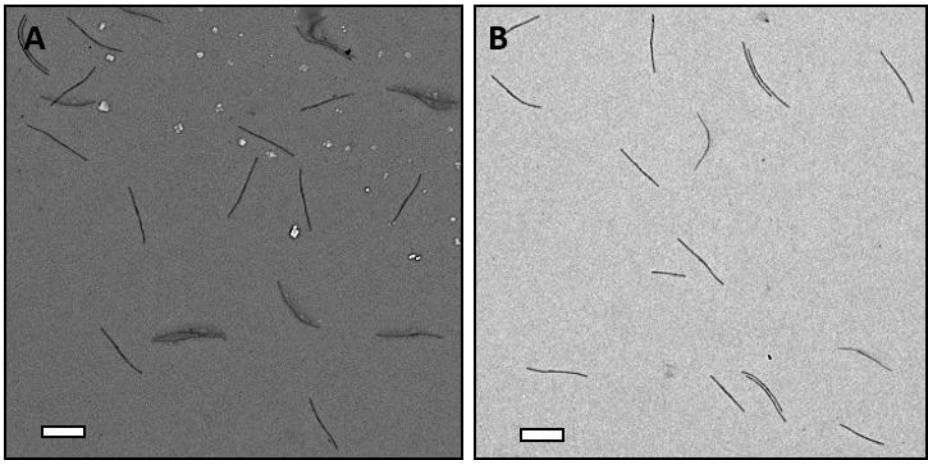

Figure S14. TEM images of micelles (c= 0.18 mg/mL) in 2-propanol before (A) and after (B) injection into 2-propanol with syringe pump (rate = 1 mL/h). Scale bars: 500 nm。

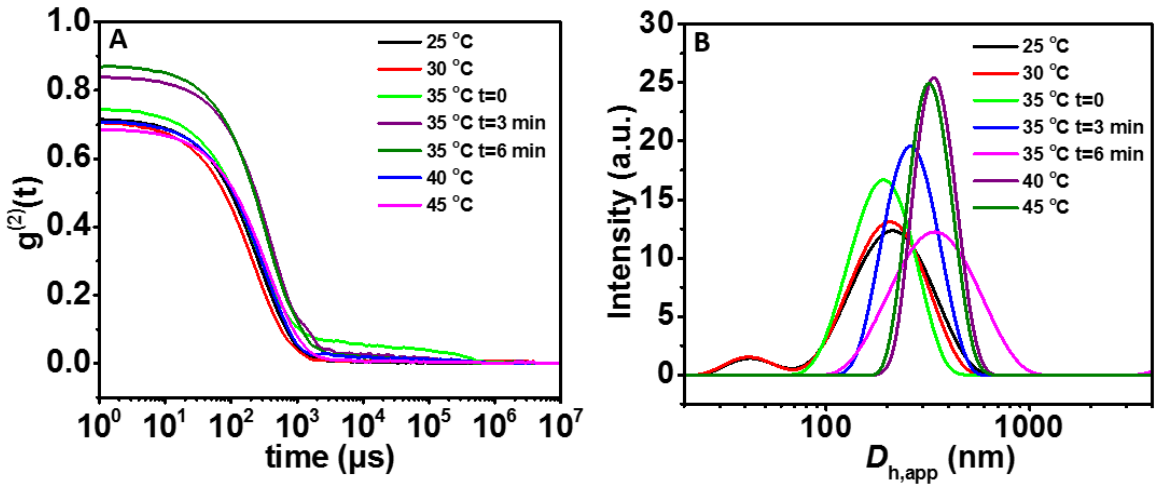

Figure S15 DLS autocorrelation function curves (A) and corresponding CONTIN plots (B) of fragmented micelles in water after equilibration for 2 mins at various temperatures.

REFERENCES

(1) Zhang, M.; Rupar, P. A.; Feng, C.; Lin, K.; Lunn, D. J.; Oliver, A.; Nunns, A.; Whittell, G. R.; Manners, I.; Winnik, M. A. Modular Synthesis of Polyferrocenylsilane Block Copolymers by Cu-Catalyzed Alkyne/Azide "Click" Reactions. *Macromolecules* **2013**, *46* (4), 1296–1304.

(2) Zhang, M. Part I: Morphology Transformation of Block Copolymer Micelles Containing Quantum Dots in the Corona. Part II: The Synthesis and Self-Assembly of New Polyferrocenylsilane Block Copolymers. Ph.D., University of Toronto (Canada): Canada, 2013.

(3) Broersma, S. Rotational Diffusion Constant of a Cylindrical Particle. *J. Chem. Phys.* **1960**, *32* (6), 1626–1631.

(4) Broersma, S. Viscous Force Constant for a Closed Cylinder. *J. Chem. Phys.* **1960**, *32* (6), 1632–1635.

(5) Broersma, S. Viscous Force and Torque Constants for a Cylinder. *J. Chem. Phys.* **1981**, *74* (12), 6989–6990.

(6) Aragon, S. R.; Flamik, D. High Precision Transport Properties of Cylinders by the Boundary Element Method. *Macromolecules* **2009**, *42* (16), 6290–6299.

(7) Guerin, G.; Qi, F.; Cambridge, G.; Manners, I.; Winnik, M. A. Evaluation of the Cross Section of Elongated Micelles by Static and Dynamic Light Scattering. *J. Phys. Chem. B* **2012**, *116* (14), 4328–4337.